



Analogue Based Design of MMP-13 (Collagenase-3) Inhibitors

J. A. R. P. Sarma,^{a,*} G. Rambabu,^b K. Srikanth,^a D. Raveendra^c and M. Vithal^{b,*}

^agvk bioSciences Pvt. Ltd., #210, My Home Tycoon, 6-3-1192, Begumpet, Hyderabad 500 016, India

^bDepartment of Chemistry, Osmania University, Hyderabad 500 007, India

^cMolecular Modeling Group, Organic Division-I, Indian Institute of Chemical Technology, Hyderabad 500 007, India

Received 23 May 2002; accepted 10 July 2002

Abstract—3D-QSAR studies using MFA and RSA methods were performed on a series of 39 MMP-13 inhibitors. Model developed by MFA method has a r_{cv}^2 (cross-validated) of 0.616 while its r^2 (conventional) value is 0.822. For the RSA model r_{cv}^2 and r^2 are 0.681 and 0.847, respectively. Both the models indicate good internal as well as external predictive abilities. These models provide crucial information about the field descriptors for the design of potential inhibitors of MMP-13.

© 2002 Elsevier Science Ltd. All rights reserved.

The matrix metalloproteinases (MMPs) are a well-studied family of endoproteinases responsible for degradation of the structural extra cellular matrix (ECM) components, such as interstitial and basement membrane collagens, fibronectin and laminin.^{1,2} This family of enzymes includes collagenases, gelatinases and stromelysins. MMPs are necessary for tissue remodeling and the healing cascade.^{3,4} However, the over expression of MMP activity or the presence of MMP activity in healthy and uninjured areas can contribute to the pathophysiology in a variety of disease states and conditions. MMP activity directed at healthy skin may be implicated in the development of psoriasis.⁵ These enzymes are apparently involved in the connective tissue degradation and are necessary for the tumor metastasis and angiogenesis. They may also play a more complicated role in the regulation and growth of tumors and the development of metastatic diseases.^{6–8}

In addition to tissue destruction and remodeling, MMPs are known to be essential for the growth of new blood vessels. Consequently, MMP inhibitors (MMPis) are under investigation for their utility in slowing or halting the progression of tumor growth and metastasis. These compounds are actively being studied by numerous groups as potentially useful new medicines.⁹ In this present study, quantitative structure activity relationship studies were carried out on a series of Collagenase-3 inhibitors, in order to design selective and potential inhibitors for Collagenase-3.⁹

3D-QSAR Studies

QSAR models were developed using Molecular Field Analysis (MFA) and Receptor Surface Analysis (RSA) methodologies using Cerius² software on a series of 39 MMP-13 inhibitors. These molecules were divided into two sets, namely the training containing 33 randomly selected molecules and a test set with six other molecules.

Molecular Structure Generation

All the molecules were modeled using a number of modules in Cerius².¹⁰ Initial conformation is obtained to be consistent with that of similar ligand in 1CAQ from the PDB. Geometric optimizations were carried out using the Drieding force field while the partial atomic charges were obtained with charge equilibration method. All the molecules were initially minimized with smart minimizer and further geometric optimizations were performed using MOPAC with the AM1 method.^{11,12} Nearly for all the molecules, the final geometry especially the central portion wherein there is maximum conformational flexibility is nearly similar to that of found for the bioactive conformation observed in 1CAQ.pdb.

Alignment

Initially, all the molecules were manually aligned to the most active molecule, **4** (Table 1) by considering the significant common substructure. Further refinement in the

*Corresponding author. E-mail: sarma@gvkbio.com

alignment was carried out by an RMS based automated approach using the molecular shape analysis (MSA) of the QSAR module.¹⁰ A stereo view of the aligned molecules are observed in Figure 1.

MFA

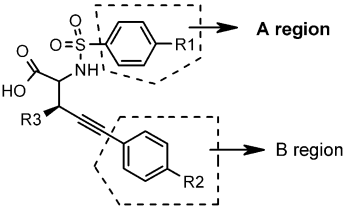
Molecular field values were generated for all the aligned molecules using CH₃ and H⁺ probes for steric and electrostatic interactions respectively using default grid values of 2 Å. Only 10% of the total variables, whose variance is highest, were considered as independent variables. The negative logarithm of the biological activities of all 33 molecules in the training set were chosen as the dependent variables (Tables 1 and 2). By using genetic function algorithm (GFA) regression method (only linear terms are considered),¹³ multiple QSAR equations were generated from which one the equation with highest r^2 and r_{cv}^2 , F -test values and low-

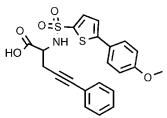
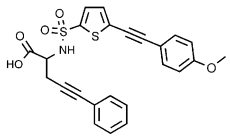
est PRESS value was considered for further discussion. The rectangular box giving the extent of fields considered are given in Figure 1.

RSA

The aligned molecular aggregate was reconsidered for the generation of receptor surface, which in principle represent a virtual active site of the target.^{14,15} The receptor surface was generated with weights based on the biological activity data. The interaction energies of all the molecules were evaluated within this receptor surface. The receptor surface descriptors, expressed as 3D-field descriptors, were derived from the van der Waals and electrostatic interaction energies between the receptor surface and CH₃ and H⁺ groups as probes. Figure 2 is a stereo view of the receptor surface also showing the molecules in the training set. These descriptors were used as independent variables for the

Table 1. MMP-13 inhibitors with observed and calculated biological activities possessing the following basic structure



Compd	R ₁	R ₂	R ₃	Activity (–log IC ₅₀)		
				Observed	Calculated	
					MFA	RSA
1	–O-nBu	H	H	–3.310	–3.372	–3.473
2	–OPh	H	H	–3.330	–3.546	–3.271
3	–Ph(4-F)	H	H	–2.360	–2.096	–1.788
4	–Ph(4-OMe)	H	H	–1.320	–1.632	–2.041
5	–Ph(4-OMe)	<i>meta</i> -N(CH ₂ CH ₂) ₂ O <i>para</i> -N(CH ₂ CH ₂) ₂ O	H	–1.380	–1.549	–1.530
6	–Ph(4-OMe)		H	–2.480	–2.305	–1.977
9	–Ph(4-SMe)	H	–OMe	–1.520	–1.534	–1.668
10	–Ph(4-OMe)	H	–OBn	–1.150	–1.767	–1.774
12	–Ph- <i>O</i> -Ph	H	H	–3.330	–3.261	–3.266
13	–Ph(3,4-OCH ₂ O-)	H	H	–2.020	–1.831	–1.588
14	Biphenyl	H	H	–1.770	–2.819	–2.181
15	–≡–Ph	H	H	–1.950	–1.741	–1.790
17	–N=N-Ph	H	H	–2.690	–2.343	–2.837
18	–NHCOPh(4-Cl)	H	H	–2.100	–1.769	–1.831
19				–1.520	–1.730	–1.426
20				–2.160	–1.932	–2.273
Test set						
7	–Ph(4-SMe)	H	H	–1.200	–1.491	–1.587
8	–Ph(4-OMe)	H	–OMe	–1.910	–1.741	–1.784
11	–Ph(4-O(CH ₂) ₂ OMe)	H	H	–1.690	–0.720	–0.982
16	–≡–Ph(4-OMe)	H	H	–1.540	–0.016	–0.928

$$n = 33, r^2 = 0.822, r_{cv}^2 = 0.616, F = 19.98, \text{PRESS} \\ = 6.993$$

$$n = 33, r^2 = 0.847, r_{cv}^2 = 0.681, F = 19.80, \text{PRESS} \\ = 5.800$$

Reasonably good values of r^2 and low Predicted Residual Error of Sum of Squares (PRESS) for the above QSAR equation explains satisfactorily the variances in the activity and good r_{cv}^2 and F values would indicate that the equation can be used to predict activities of new molecules with reasonable accuracy. Eq 1 consists of six molecular field descriptors (from top to the bottom) namely, CH₃/1138, H⁺/1279 and 1307 in the **A** region; CH₃/404, H⁺/532 and 714 in the **B** region. The positive coefficient of CH₃/1138 descriptor indicate bulky substituents like bulky meta substituent phenyl rings attached to propargyl group expected to be more favourable for improving the activity. Further, the interior position of the 1138 grid point would indicate, further enhancement of the activity with bulky group substitution in vicinity of that region. Electrostatic interactions at the grid points H⁺/1279 and 1307 indicate that the biological activity can be enhanced with negative charge in the central portion of region **A**. Perhaps, this would indicate that oxygen substitution in the form of morpholine, OMe and other ether groups contribute to such an effect. Electrostatic interactions in the grid points of 532 and 714 in the **B** region indicate electropositive substitutions are important to enhance the activity, while bulky group substitution near this region (indicated by the grid point 404) has a negative effect on the activity. Many anisole, thioanisole, biphenyl and other substitutions explain such features. However, extending the substitution by three rings, *meta*- or *para*-lengthy substitutions have negative effect on the activity. The predictive ability of this MFA model was evaluated by predicting the biological activities of the test set molecules. The predicted and actual activities of the training set and test set molecules are given in Tables 1 and 2. Figure 1 is the stereo view of the molecules in the training set with a rectangular field grid. Only those field points involved in the QSAR equation are shown in Figure 1.

RSA

The QSAR model generated by using RSA is represented as eq 2:

$$\text{Activity} = -8.6292 + 13.7223 * \text{ELE4400} + 1079.4 \\ * \text{VDW/5505} + 14.1436 \text{VDW/5957} \\ + 15.2277 * \text{ELE2250} - 10.5360 \\ * \text{ELE3193} - 3.9100 * \text{VDW/4887} \\ - 1074.5700 * \text{VDW/5513} \quad (2)$$

The above equation explains 84.70% of variances in the activity. Although r^2 and F values are nearly comparable with those of MFA model, the lower PRESS value as well as improved cross-validated r^2 value in this case, indicate a better predictivity compared to MFA model. From eq 1, the positive coefficient of VDW/5957 descriptor in the **B** region explains that a linear bulky group at R1 position improves the activity. This is clear from the activities of the different compounds. The compounds with the linear substitutions, are shown to be oriented towards VDW/5957 and have better activities when compared to the non-linear groups. N and O atoms, present in the middle of the bulky group in molecules for example **2** and **26**, cause a orientation change and reduce the activity. The descriptor ELE/2250 explains the requirement of more electropositive groups at interior portion of **A** region, that is at the *meta* position of phenyl ring attached to the propargyl group. This is clearly observed in the activities of compounds **5** and **6**. ELE/3193 explains the improvement in activity by putting more electronegative groups at the exterior of the **A** region about the phenyl ring. The descriptor ELE/4400 explains the possibilities of improving the activity with some electropositive substituents over an aromatic ring attached to –SO₂ at **B** region. Predictive ability of this model was evaluated by predicting the biological activities of the test set molecules and the actual, predicted activities are given in Tables 1 and 2. The violet and green colors in Figure 2 indicate the favorable and unfavorable interactions respectively, between the molecules and the receptor surface while the grey region indicate the subtle variation in the energy between receptor surface and the molecules under consideration and could suggest a greater flexibility in the conformational as well as substitutional implications.

Conclusion

The RSA model has shown to predict better when compared with MFA. Even though models infer similar information about the substitutional requirements for the better activities, in general the RSA model agree well with the experimental results in the test set as well as in the training set. The middle portion of the aligned molecules is conserved which is responsible for their binding with Zn atom in matrix metallo proteins (MMP) where as flexibility is allowed in **A** and **B** regions for better activity.

References and Notes

1. Morphy, J. R.; Millican, T. A.; Porter, J. R. *Curr. Med. Chem.* **1995**, 2, 743.

2. Matrisian, L. M. *Bioessays* **1992**, *14*, 455.
3. Buisson, A. C.; Gilles, C.; Polttte, M. *Lab. Invest.* **1996**, *74*, 658.
4. Buisson, A. C.; Zahm, J. M.; Polette, M.; Pierrot, D.; Bel-lon, G.; Puchelle, E.; Birembaut, P.; Tournier, J. M. *J. Cell. Physiol.* **1996**, *166*, 413.
5. Holleran, W. M.; Galardy, R. E.; Gao, W. N.; Levy, D.; Tang, P.; Elias, P. M. *Arch. Dermatol. Res.* **1997**, *289*, 138.
6. Bramhall, S. R. *Int. J. Pancreat.* **1997**, *21*, 1.
7. Lafleur, M.; Underwood, J. L.; Rappolee, D. A.; Werb, Z. *J. Exp. Med.* **1996**, *184*, 2311.
8. Wojtowicz-Praga, S. M.; Dickson, R. B.; Hawkins, M. J. *Invest. New Drugs* **1997**, *15*, 61.
9. Michael, G. N.; Roger, G. B.; Matthew, J. L.; Staszek, P.; Neil, G. A.; Biswanath, D.; Michael, J. J.; Lily, C. H.; Fei, G.; Matthew, E. P.; Vikram, S. P.; Susan, M. G.; Sean, X. P.; Todd, M. B.; Selane, L. K.; Timothy, R. B.; David, J. F.; Glen, E. M. *J. Med. Chem.* **2001**, *44*, 1060.
10. Cerius 2 Aprogram Suite for Molecular Modelling Activ-ities; Molecular Simulations: Scranton Raod, San Diego, CA 92121–3752, USA.
11. Stewart, J. J. S. *J. Comput.-Aided Mol. Des.* **1990**, *4*, 1.
12. Dewar, M. J. S.; Zoeebish, E. G.; Healy, E. F.; Stewart, J. J. P. *J. Am. Chem. Soc.* **1985**, *107*, 3902.
13. Rogers, D.; Hopfinger, A. J. *J. Chem. Inf. Comput. Sci.* **1994**, *34*, 854.
14. Hahn, M. *J. Med. Chem.* **1995**, *38*, 2080.
15. Hahn, M.; Rogers, D. *J. Med. Chem.* **1995**, *38*, 2091.